

# Semiconductor Electrodes

## XXXIII. Photoelectrochemistry of n-Type WSe<sub>2</sub> in Acetonitrile

Henry S. White, Fu-Ren F. Fan, and Allen J. Bard\*

Department of Chemistry, The University of Texas at Austin, Austin, Texas 78712

### ABSTRACT

The photoelectrochemical behavior of n-type WSe<sub>2</sub> single crystal electrodes in acetonitrile solutions containing several redox couples ( $I^-/I_3^-$ ,  $Br^-/Br_2$ ,  $Cl^-/Cl_2$ , thianthrene<sup>0/+</sup>,  $Ru(bpy)_3^{2+/3+}$ ) was investigated. Electrodes with discontinuities in the van der Waals' surface show large dark currents and recombination of electrons with photo-oxidized solution species. Pretreatment of such a surface with  $Cl^-$  passivates these dark active sites and increases the photocurrent density. The observed photopotentials at WSe<sub>2</sub> for redox couples with potentials,  $V_{redox}$ , more positive than 0.5V vs. SCE show behavior consistent with Fermi level pinning; the onset potential of photocurrents increases linearly with increasing  $V_{redox}$  while the photopotential remains constant. The energy position at which pinning occurs depends on the density of surface states and the concentration of solution species. The characteristics of a photovoltaic cell based on the n-WSe<sub>2</sub>/Cl<sup>-</sup>, Cl<sub>2</sub><sup>-</sup>/Pt system is also described.

The performance of photoelectrochemical devices for conversion of solar to chemical and electrical energy can be critically limited by processes occurring via intermediate energy levels at the semiconductor/liquid interface (surface states). Surface recombination and Fermi level pinning are two such processes that generally are detrimental to efficient energy conversion. In either case the photoelectrochemical results are somewhat different from expectations based on the idealized model (1) of the semiconductor electrode/solution interface. A number of investigations of the dependence of potential distribution (2) and charge transfer kinetics (3) on surface states have been carried out. The surface pretreatment or modification procedures can influence the distribution and density of surface states at energies located within the band-gap and thus cause changes in the electrochemical behavior (4, 5).

Recently, Tributsch and co-workers have introduced photoelectrochemical cells based on layer-type transition metal dichalcogenides (5). These and later investigations (6-11) have shown that the observed photopotentials in aqueous (5f, 9) and nonaqueous (6-8) solutions are smaller than the expectations based on the ideal junction model. Lewerenz (10) and Tributsch (11) and co-workers have also recently investigated the role of surface morphology on conversion efficiencies of layered semiconductors in aqueous solutions. We report here an investigation of n-type WSe<sub>2</sub> electrodes in acetonitrile (MeCN) solutions. The effect of the nature of the surface and pretreatment procedures on the electrochemical response and a photovoltaic cell based on the photogeneration of chlorine at n-type WSe<sub>2</sub> immersed in an MeCN solution containing  $Cl^-/Cl_2$  is described.

### Experimental

**Semiconductor electrodes.**—N-type WSe<sub>2</sub> single crystals were generously donated by Dr. Barry Miller and Dr. Frank DiSalvo of Bell Laboratories. Electrical contacts were made to the back of each crystal by rubbing In/Ga alloy into the crystal to which a copper lead was contacted with silver epoxy cement (Allied Products Corporation, New Haven, Connecticut). A clean new crystal face ( $\perp$  C-axis) was exposed by sticking adhesive tape on the front side and gently pulling off the top surface layer. To obtain electrodes with only

the van der Waal's surface ( $\perp$  C-axis) exposed, a very minute surface area was carefully chosen that was free from any edges or face defects; these are known to provide recombination centers (10, 11). Such electrodes are designated "type S" in this paper. No electrodes were prepared with only the surface  $\parallel$  C-axis exposed, since the crystals were only  $\sim 1$ -2 mm thick along this plane and are difficult to mount without leaking. Electrodes were prepared from several crystals that had visible edges (discontinuities in the otherwise smooth van der Waal's plane) exposed to the solution. These electrodes are designated "type E." Scanning electron micrographs of type S and type E WSe<sub>2</sub> electrodes are shown in Fig. 1. The surface defects represented roughly 5%-10% of the total surface area of type E electrodes.

The crystal sides and back and the copper lead were completely covered with 5 min epoxy cement; this was then covered with silicone rubber sealant (Dow Corning Corporation, Midland, Michigan). For long-term stability measurements involving strong oxidants, such as  $Cl_2$ , the electrode was covered with a preactivated photo-cure epoxy cement that is used in dental restorative work (Caulk Nuva-Fil, D.A., Milford, Delaware). The exposed areas of the crystal faces in both types of electrodes were between 0.010 and 0.070 cm<sup>2</sup>.

Unless noted otherwise, before each experiment the electrodes were etched in 12M HCl for 15-30 sec, rinsed thoroughly with distilled water, and dried under vacuum for 1 hr. The electrodes were then stored inside an He-filled dry box (Vacuum Atmospheres, Hawthorne, California) and used within one day.

**Chemicals.**—All electrochemical grade tetraalkylammonium salts were purchased from Southwestern Chemical Company (Austin, Texas). Tetrabutylammonium perchlorate (TBAP), tetrabutylammonium bromide (TBABr), tetramethylammonium chloride (TMACl), and tetrabutylammonium iodide (TBAI) were crystallized at least twice from acetone-ether and dried under vacuum for 2 days. Tetraethylammonium chloride (TEAC) was recrystallized from MeCN-ether and dried as above. Thianthrene (Th) (Aldrich Chemicals) was either sublimed three times or recrystallized from benzene twice.  $Ru(bpy)_3(ClO_4)_2$  was prepared and purified as previously described (12). After purification the reagents were stored inside the dry box.  $I_2$  (Fisher Scientific Company),  $Br_2$  (MCB), and  $Cl_2$  (Matheson Gas Company) were used without

\* Electrochemical Society Active Member.

Key words: capacitance, voltammetry, photopotential, oxidation, solar cells.

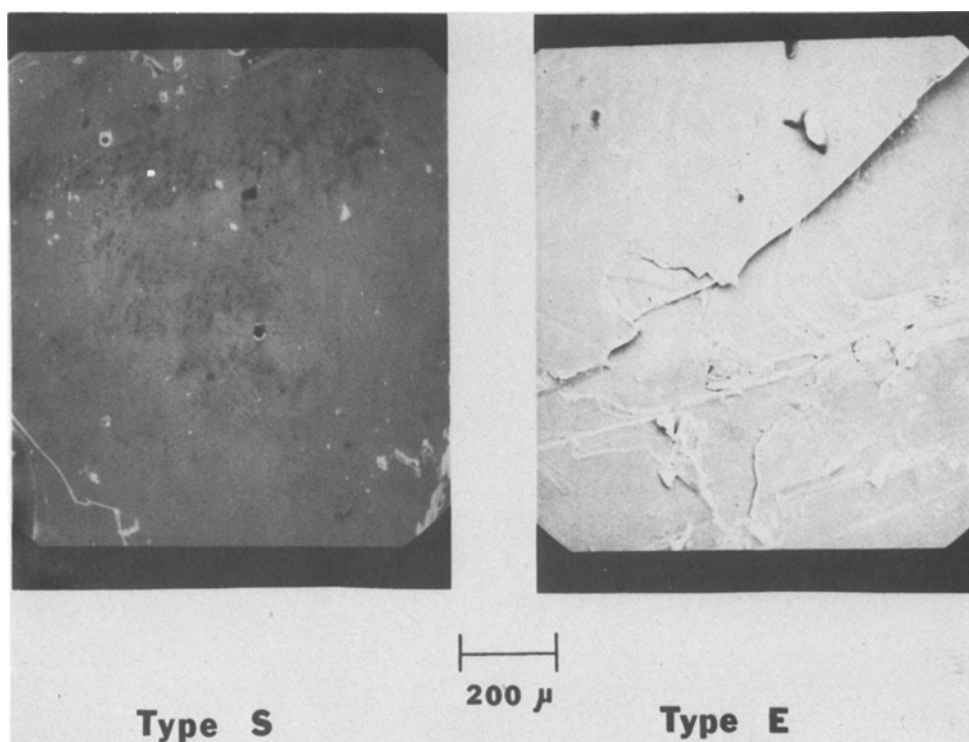


Fig. 1. Scanning electron micrographs of  $WSe_2$  electrodes: (a) type E; (b) type S. Magnification  $100\times$ .

further purification. MeCN was purified and dried as previously described (13) and stored inside the dry box.

**Electrochemical apparatus.**—Voltammetric measurements were made in a two-compartment cell (30 ml) equipped with an optically flat Pyrex window. The working and reference electrodes were separated from the auxiliary electrode, a Pt flag ( $\sim 8\text{ cm}^2$ ), by a medium-porosity frit. Along with the semiconductor electrodes the main compartment contained a Pt disk ( $0.025\text{ cm}^2$ ) sealed in glass that was used to check the purity of the electrolyte and to locate the potential of the reference electrode with respect to the potential of a known reversible redox couple. The reference electrode was a polished silver wire inside a glass cylindrical compartment containing only the supporting electrolyte and separated from the main solution by a medium-porosity frit. All potentials reported here are referenced to an aqueous saturated calomel electrode (SCE). Single compartment, two-electrode cells, also equipped with optically flat Pyrex windows, were used as photovoltaic (solar) cells.

The electrochemical cell and solutions were prepared before each experiment within the dry box. All ground glass joints were sealed with silicone-based vacuum grease to permit the cell to be removed from the inert atmosphere for study. When the experiment required opening of the electrochemical cell outside of the dry box, prepurified  $N_2$  was blown over the top of the solution until the cell was reclosed.

The cyclic voltammograms were obtained with a Princeton Applied Research (PAR) Model 173 potentiostat and PAR Model 175 Universal programmer and recorded on a Houston Instruments Model 2000 X-Y recorder. Capacitance measurements were made using a PAR Model HR-8 lock-in amplifier. Solar cell current-voltage curves were made by measuring the voltage across a variable load resistance with a Keithley Model 179 TRMS digital multimeter.

The light source used for photoelectrochemical studies was an Oriel Corporation (Stamford, Connecticut) 450W xenon lamp. A red filter was used to eliminate wavelengths below 590 nm. Neutral density filters (Oriel Corporation) were used to vary the light intensity. The full, filtered xenon lamp power output was  $\sim 150\text{ mW/cm}^2$  as measured with an E. G. and G.

(Salem, Massachusetts) Model 550 radiometer/photometer and a Scientech 361 power meter.

## Results

**Capacitance measurements and cyclic voltammetry in the absence of redox couple.**—Capacitance measurements on several n- $WSe_2$  electrodes in MeCN containing only TBAP (0.2M) resulted in two distinct types of behavior. The capacitance vs. potential curve of a type S electrode, Fig. 2, closely resembles behavior typical of a fairly large bandgap n-type semiconductor, where at potentials positive of the flatband potential,  $V_{FB}$ , the space charge region is depleted of electrons and contains ionized donors at some constant concentration (1). This region extends up to potentials of 1.3V vs. SCE. At potentials more negative than  $-0.4V$ , the capacitance becomes constant indicating the onset of degeneracy. The voltammetric behavior of the same electrode in MeCN-0.2M TBAP is shown in Fig. 3. In the dark a small current,  $\sim 0.2\text{ mA/cm}^2$ , begins at 0.6V. Under illumination, the photocurrent begins at  $\sim 0.5V$  and increases steadily at more positive potentials. At  $\sim 1.0V$ , the photocurrent is  $\sim 1.0\text{ mA/cm}^2$ . On the reverse

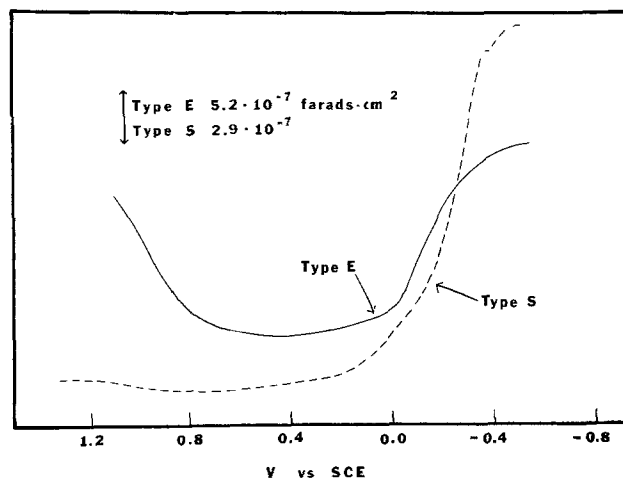


Fig. 2. Differential capacitance curve for type E and type S  $WSe_2$  electrodes in MeCN containing 0.2M TBAP. Scan rate, 5 mV/sec; applied a-c voltage, 5 mV rms. Frequency, 1000 Hz.

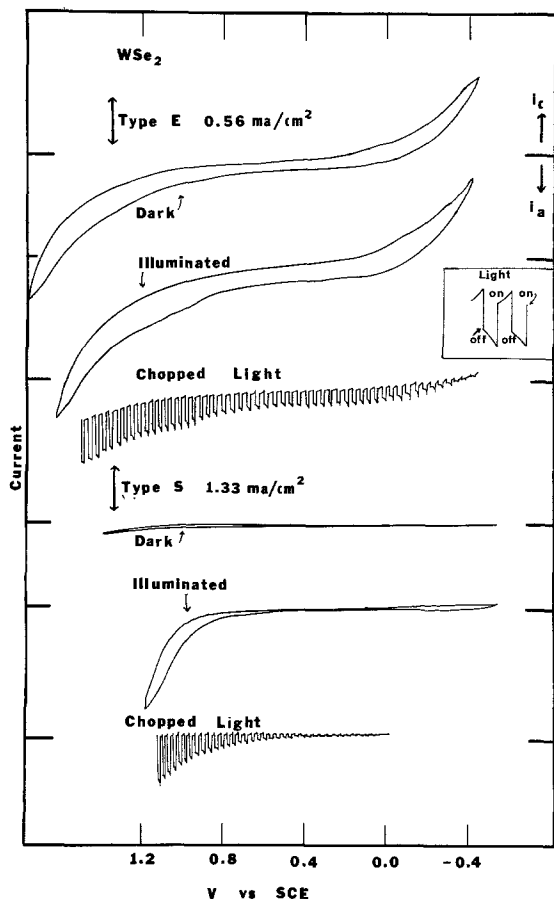


Fig. 3. Voltammetric behavior of type S and type E electrodes in MeCN-0.2M TBAP. Scan rate, 100 mV/sec, except for chopped light scans, 10 mV/sec.

scan, under illumination, a small cathodic current,  $\sim 0.2$  mA/cm<sup>2</sup>, begins at 0.0V. This same cathodic current is observed if the light is turned off on the reverse scan and increases with more positive switching potentials. The anodic photocurrent and induced dark current are probably due to the oxidation and re-reduction of the crystal surface caused by traces of H<sub>2</sub>O in the acetonitrile (5e). Further purification of the solvent by addition of Al<sub>2</sub>O<sub>3</sub> significantly reduced these currents.

The capacitance behavior of a type E WSe<sub>2</sub> electrode, also shown in Fig. 2, is typical of electrodes with discontinuities in the van der Waal's surface. The branch toward negative potentials is similar in shape to the type S electrodes. However, at potentials more positive than 0.7V, the capacitance increases sharply indicating either deep surface states, inversion of the space charge region, or the occurrence of a faradic process.

As Tributsch has already pointed out (5e), inversion of the space charge region in a semiconductor with a bandgap of 1.4 eV is unlikely within this potential region. If space charge inversion due to thermal activation of electrons into the conduction band were responsible for this increase in capacitance, both type S and type E electrodes should show this behavior. The voltammetric behavior of the same crystal (type E) in a blank solution is shown in Fig. 3. A dark anodic current is observed that is approximately five times larger than on the type S electrode (compare at 1.0V). Under illumination, a photocurrent begins at  $-0.3$ V and is fairly constant until 0.7V where a sharp increase in anodic currents begins. The net photocurrent density at 1.0V is  $\sim 0.6$  mA/cm<sup>2</sup>, which is  $\sim 60\%$  the current density at the type S electrode. The  $V_{FB}$  values and donor densities of these crystals were estimated from the capacitance measurements. Mott-Schottky plots for the two crystals described above are shown in Fig. 4a and 4b. The results for several crystals are summarized in Table I.  $V_{FB}$ , for WSe<sub>2</sub> in MeCN, estimated by extrapolating to the potential where  $1/C_{sc}^2 = 0$ , was always in the range of  $-0.2$  to  $-0.4$ V vs. SCE. The apparent donor densities,  $n_D$ , for type E electrodes were 3-7 times larger than for type S electrodes. As can be seen in the Mott-Schottky plots, the apparent capacitance values were highly dependent on the frequency of the applied alternating voltage. Frequency dispersion of the capacitance due to dielectric relaxation should be negligible in a covalent-type material like WSe<sub>2</sub>. It is possible that the dispersion observed here is due to small changes in the effective electrode surface due to corrosion. The values of  $n_D$  listed in Table I are from measurements in the range 500-1000 Hz. A value of 10 for the dielectric constant of WSe<sub>2</sub> was used in all calculations (14).

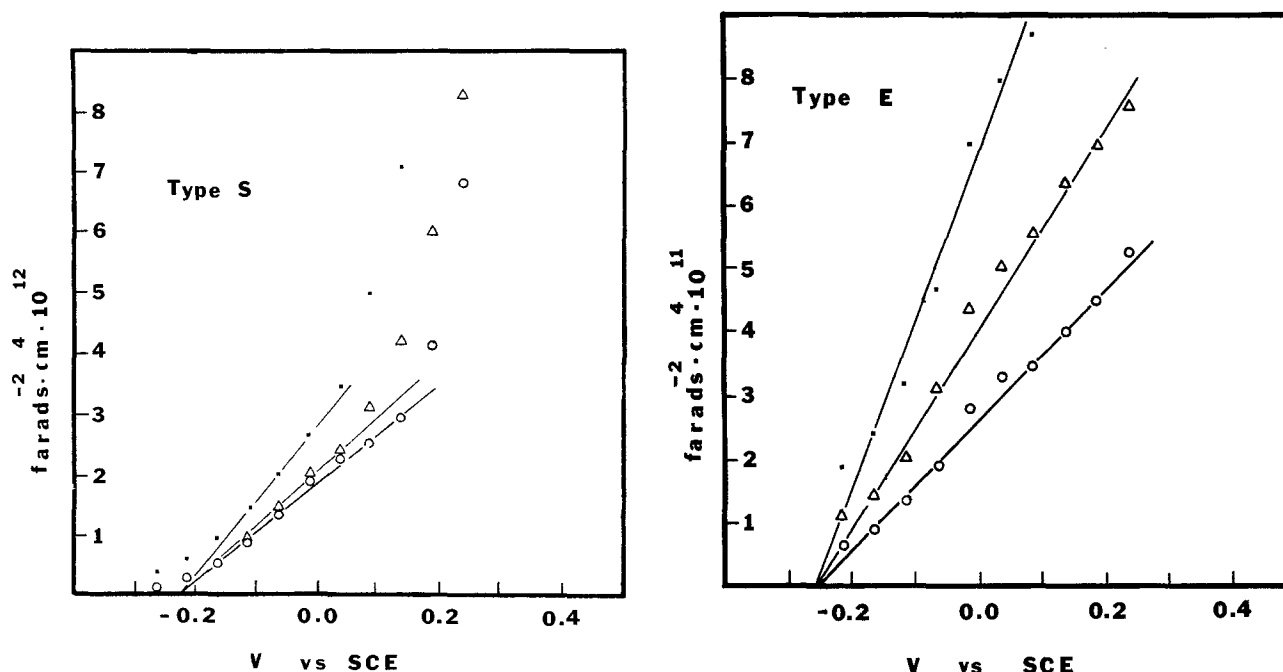


Fig. 4. Mott-Schottky plots of (a) type S and (b) type E WSe<sub>2</sub> electrodes in MeCN-0.2M TBAP. (○) 200 Hz, (△) 500 Hz, (■) 1000 Hz

Table I. Estimates of flatband potentials and donor densities for n-WSe<sub>2</sub>

Crystal, WSe <sub>2</sub>	V <sub>FB</sub> (V vs. SCE)	n <sub>D</sub> (cm <sup>-3</sup> )
Type S	-0.22	1.3 × 10 <sup>18</sup>
	-0.36	2.0 × 10 <sup>18</sup>
	-0.42	1.8 × 10 <sup>18</sup>
Type E	-0.26	8.5 × 10 <sup>18</sup>
	-0.4*	5.6 × 10 <sup>18</sup>

\* Measured vs. Ag quasi-reference electrode and corrected to SCE with accuracy of  $\pm 0.1V$ .

**Voltammetric behavior of various redox couples at n-WSe<sub>2</sub>.**—Types S and E electrodes showed distinctly different voltammetric behavior. Recall that type E electrodes are those that have visible edges or discontinuities in the van der Waal's plane exposed to the solution. These edges have been associated with the face parallel to the main C-axis (|| C-axis) (15) where empty conduction band orbitals are exposed to the solution. The results are summarized in Tables II and III.

**Oxidation of I<sup>-</sup> and Br<sup>-</sup>.**—The type S electrode shows negligible dark current in the vicinity of I<sup>-</sup> oxidation on Pt (Fig. 5a). Upon illumination, the potential for onset of photocurrent, V<sub>on</sub>, was 0.0V and attains a saturation current at  $\sim 0.2V$ . The chopped light voltammogram clearly indicates that little back-reaction (reduction of photo-oxidized products) occurs beyond the onset potential. The dark current at the type E electrode in the presence of I<sup>-</sup> (Fig. 5b) was smaller (i.e., about one-tenth) than in the blank solution (Fig. 3). V<sub>on</sub> was  $\sim 0.07V$  more negative than the V<sub>on</sub> at the type S electrode. This difference in onset potential is approximately the difference in the measured flatband potentials for these crystals. The maximum photocurrent densities were about the same for both type S and type E electrodes. However, on scan reversal, a much larger reduction peak centered at  $-0.07V$  was found with the type E electrode.

The oxidation of Br<sup>-</sup> (as TBABr) on WSe<sub>2</sub> followed behavior similar to that found for I<sup>-</sup> (Fig. 6a and 6b).

Table II. Voltammetric data for various redox couples at WSe<sub>2</sub>

Couple	Pt*		Type S**		Type E†	
	V <sub>pa</sub>	V <sub>pc</sub>	V <sub>onset</sub>	V <sub>pc</sub>	V <sub>onset</sub>	V <sub>pc</sub>
I <sup>-</sup> /I <sub>3</sub>	0.35	0.1	0.00	—	-0.07	-0.08
Br <sup>-</sup> /Br <sub>2</sub>	0.69	0.25	0.05	-0.35	0.02	-0.12
Cl <sup>-</sup> /Cl <sub>2</sub>	1.09	0.82	0.55	—	0.21	-0.02
Th <sup>0/+</sup>	1.26	1.20	0.60	0.76	0.67	0.75
Ru(bpy) <sub>3</sub> <sup>2+/3+</sup>	1.33	1.27	0.91	0.96	—	—

\* All values in V vs. SCE; E<sub>onset</sub> = potential of photocurrent onset.

\*\* Under illumination; negligible dark anodic currents at type S electrodes.

† Under illumination; no well-defined peaks in dark except for thianthrene oxidation, V<sub>pa</sub> = 1.35V; V<sub>pc</sub> = 1.15V.

Table III. Comparison of current densities at type S and type E WSe<sub>2</sub> electrodes in solutions containing various redox couples

Redox couple	Current, * mA/cm <sup>2</sup>			
	Type S		Type E	
	Dark*	Illuminated	Dark	Illuminated
I <sup>-</sup>	<0.1	0.66	<0.1	0.71
Br <sup>-</sup>	<0.1	5.0	<0.1	1.1
Cl <sup>-</sup>	<0.1	6.0	0.1	2.0
Th	<0.1	3.2	2.4	2.4

\* Dark current measured at potential of oxidation peak on Pt. Photocurrent measured at peak potential for type E electrodes. Measured at current plateau for type S electrode except for Br<sup>-</sup> where i<sub>photo</sub> was measured at 0.8V.

The V<sub>on</sub> for the type E electrode was about 30 mV more negative than for the type S electrode. A much larger difference existed, however, in the total photocurrent densities. The current density at the type S electrode was about 4-5 times larger than that at type E.

**Oxidation of Cl<sup>-</sup>.**—The voltammetric behavior for the oxidation of Cl<sup>-</sup> at the two WSe<sub>2</sub> electrodes are shown in Fig. 7a and 7b. At the type S electrode, V<sub>on</sub> is 0.55V. Again, no dark current or back-reaction is seen at this electrode. The oxidation of Cl<sup>-</sup> on the type E electrode is strikingly different. V<sub>on</sub> was 0.34V more negative at this crystal. This difference in onset potential cannot be accounted for by the small difference in flatband potential ( $\sim 50$  mV). The cyclic voltammogram at the type E electrode shows a large reduction peak centered at 0.17V in the dark on scan reversal. This peak probably corresponds to the reduction of chlorine generated in the dark on the anodic scan. Under illumination, this reduction peak occurred at a potential about 0.2V more negative. No reverse reduction peak was observed in the dark on the type S electrode since no dark anodic current flowed. However, under illumination, a similar cathodic current was observed at potentials more negative than 0.0V.

**Thianthrene.**—The voltammetric behavior for the oxidation of thianthrene (Th) at the two WSe<sub>2</sub> crystals is shown in Fig. 8a and 8b. While under illumination, the onset potential and waveforms are almost identical at the two electrodes; in the dark a striking difference exists. With the type E electrode, a large quasi-reversible peak is located at approximately the same potential as on Pt. The current density in the dark is equal to the photocurrent density. On the type S electrode, no dark anodic current is observed. On scan reversal following an anodic scan under illumination, a cathodic peak is observed at both type E and S electrodes.

**Oxidation of thianthrene in the presence of halide.**—The photo-oxidation of Th with small amounts of halide species (10-15 mM) added to the solution was studied to determine the effect of halide ions on the photoelectrochemical behavior of WSe<sub>2</sub>. The cyclic voltammograms obtained in the dark at the type E electrode in mixed Th/halide solutions is shown in Fig. 9. The previously observed dark quasi-reversible wave

due to Th oxidation and Th<sup>•+</sup> reduction is noticeably absent in the presence of I<sup>-</sup>, Br<sup>-</sup>, or Cl<sup>-</sup>. A comparison of the cyclic voltammograms under illumination of thianthrene alone and with either I<sup>-</sup> or Br<sup>-</sup> in solution shows little change in the peak potentials due to Th photo-oxidation. In the presence of Cl<sup>-</sup>, however, these peaks, which were centered around 0.75V vs. SCE, are absent (Fig. 10), and instead, a new pair of oxidation and reduction waves centered at 0.52V appeared. These peaks were not present in solutions containing Cl<sup>-</sup> alone and therefore are assigned to the oxidation and reduction of Th. From these results, it appears that Cl<sup>-</sup> induces a 230 mV shift in V<sub>on</sub> for the oxidation of thianthrene. To demonstrate that this effect results from the interaction of Cl<sup>-</sup> with the surface discontinuities, the experiment illustrated by Fig. 11 was undertaken. A fresh type E electrode was prepared and the dark and photo-oxidation of Th was observed (curves a, b). The electrode was then removed and dipped into an MeCN solution of 7.0 mmoles TEACl in the dark without any external electrical connection. After 30 sec, the electrode was removed, rinsed thoroughly with MeCN, and placed back into the original Th-containing solution. The resulting cyclic voltammograms (curves c and d) showed an immediate decrease in the dark current and a negative shift ( $\sim 180$  mV) of the onset potential for photocurrent. The maximum photocurrent for Th oxidation increased by about 25% following this surface treatment. This improved photocurrent-potential curve re-

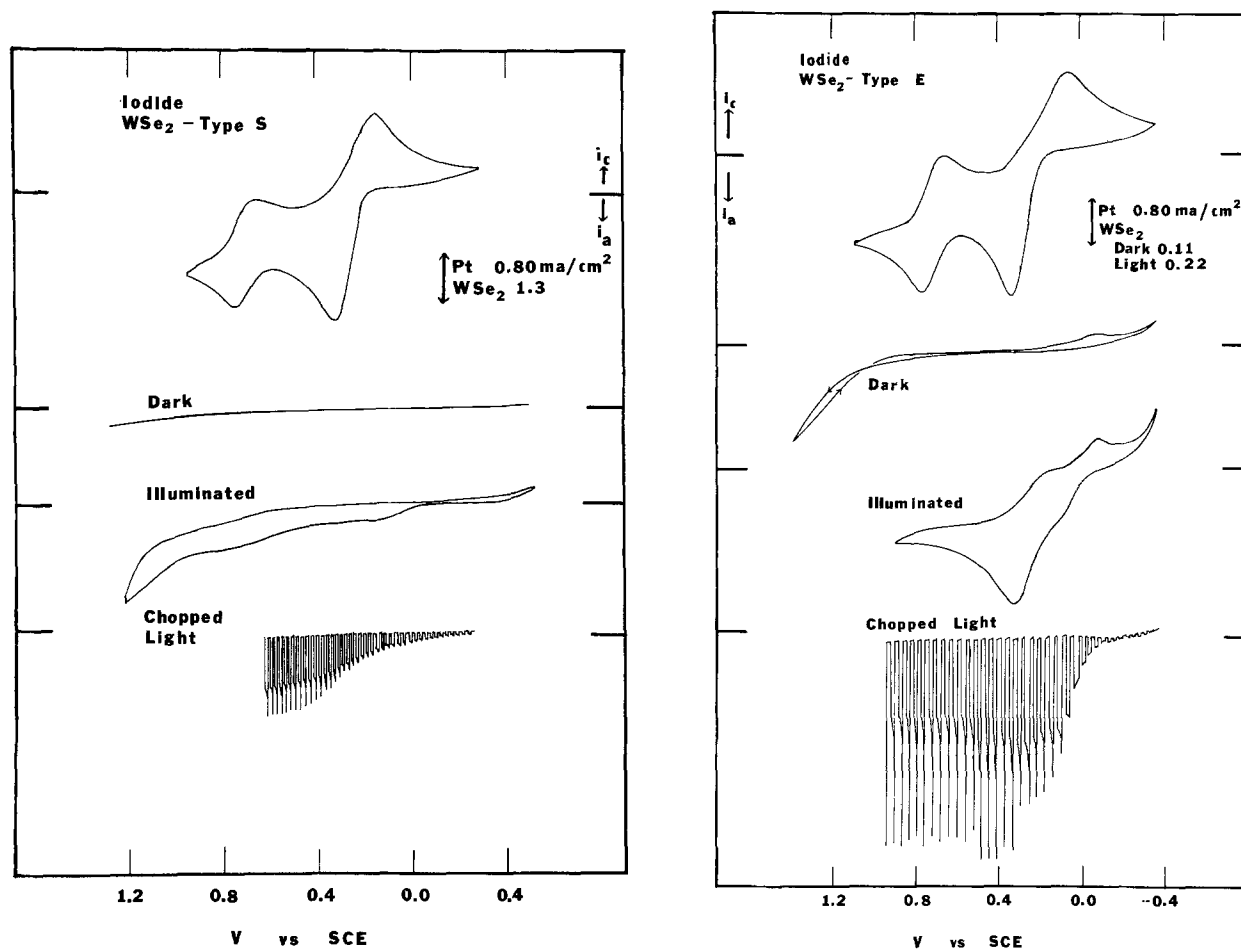


Fig. 5. Voltammetric behavior of iodide in MeCN containing 0.2M TBAP and TBAI. (a) Type S, [I<sup>-</sup>], 10 mmoles; (b) type E, [I<sup>-</sup>], 15 mM. Scan rate, 100 mV/sec, except for chopped light scan at 10 mV/sec.

mained unchanged for at least 30 min of continuous cycling. When a similar experiment was carried out with a type S electrode, no changes in the dark oxidation current (which was negligible) or the photocurrent was found by a Cl<sup>-</sup> pretreatment. Note that the decrease in dark current for the type E electrode on treatment with Cl<sup>-</sup> takes place without any possibility of photo-oxidation occurring during the exposure of the electrode to Cl<sup>-</sup> so that the formation of a light-induced complex between the electrode and Cl<sup>-</sup> is unlikely. The observed effect can be ascribed to interactions of the Cl<sup>-</sup> with surface discontinuities leading to modification or passivation of these sites.

**Photovoltaic cell based on WSe<sub>2</sub>/Cl<sup>-</sup>, Cl<sub>2</sub>, (MeCN)/Pt.**—Schneemeyer and Wrighton have previously reported photovoltaic cells based on the generation of Cl<sub>2</sub> at illuminated MoS<sub>2</sub> (6) and MoSe<sub>2</sub> (7) in MeCN. Similar cells employing type S WSe<sub>2</sub> photoanodes were constructed to test the efficiency and stability of this material. The *i*-*V* characteristics for several electrodes in cells saturated with TEACl and with Cl<sub>2</sub> bubbled through the solution are shown in Fig. 12. The open-circuit photovoltage, *V*<sub>oc</sub>, and short-circuit photocurrents, *i*<sub>sc</sub>, for several electrodes are listed in Table IV.

At low photovoltages the photocurrents at several electrodes appear remarkably high, representing quantum efficiencies of 1 (or even more) under short-circuited conditions. A sharp drop in photocurrent (~30%-40%) is observed with increasing load resistance in the first 100 mV of the photo *i*-*V* curve (Fig. 12). To determine if these unusually high currents are due to a photoinduced corrosion process, a WSe<sub>2</sub> crystal (11.5 mg) was placed in contact with a Pt electrode and immersed in a 2.0M TEAC solution saturated with Cl<sub>2</sub>. After 60 hr under illumination (~80 mW/cm<sup>2</sup>) the crystal remained unchanged with no weight loss (±0.1

mg). While this experiment may not reproduce the actual conditions of a PEC cell, photoinduced corrosion does not appear to be the major cause of the high short-circuit currents. Other causes for this result, such as the focusing or scattering of the incident radiation onto the very small area electrode by the surrounding glass or sealant to cause a higher effective light flux on the electrode, have been considered. Probing experiments with the small beam of an He-Ne laser show that this is a small effect. At this time, the actual cause of these anomalous currents is unclear.

*V*<sub>oc</sub> depended strongly on the amount of Cl<sub>2</sub> bubbled through the solution. The highest *V*<sub>oc</sub> values listed for the 1.9M Cl<sup>-</sup> solutions (Table IV) were produced by optimizing the Cl<sup>-</sup>/Cl<sub>2</sub> ratio. No attempt was made to measure exactly the amount of Cl<sub>2</sub> dissolved in the solution. As shown in Fig. 13, *V*<sub>oc</sub> drops considerably as excess Cl<sub>2</sub> is added to the solution. In a regenerative photocell with an inert metal electrode and without an external power supply the photocurrent can be limited by either processes at the photoanode or at the metal cathode. Thus, at low concentrations of Cl<sub>2</sub> the photocurrent was limited by mass transfer to the platinum cathode, while at high Cl<sub>2</sub>/Cl<sup>-</sup> ratios, the photovoltage was limited by the solution redox potential (as discussed below). When the photocurrent did not increase with higher concentrations of Cl<sup>-</sup> or Cl<sub>2</sub>, addition of Cl<sup>-</sup> to the solution increased *V*<sub>oc</sub>. The *i*<sub>sc</sub> value increased steadily with Cl<sup>-</sup> concentration up to 1.6M. Additional increases in Cl<sup>-</sup> concentration had no effect on *i*<sub>sc</sub> or *V*<sub>oc</sub>.

In a 1.9M Cl<sup>-</sup> solution, *V*<sub>oc</sub> approached a constant maximum value at light intensities ≥30 mW/cm<sup>2</sup>. The short-circuit photocurrent increased linearly with light intensity up to 120 mW/cm<sup>2</sup>, where it also reached a saturation value.

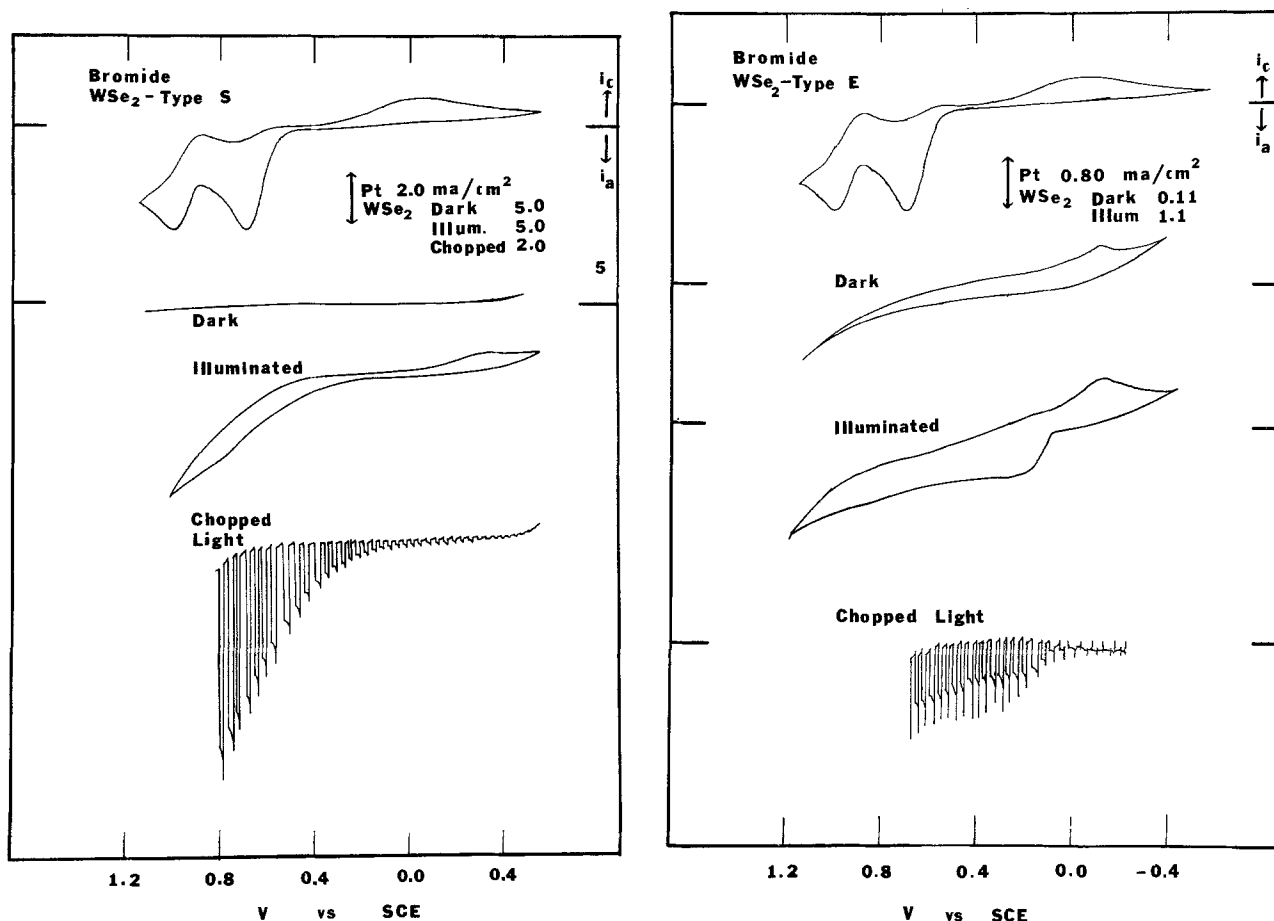


Fig. 6. Voltammetric behavior of bromide in MeCN containing 0.2M TBAP and 10 mM  $\text{Br}^-$ . (a) Type S; (b) type E. Scan rate, 100 mV/sec except for chopped light scan at 10 mV/sec.

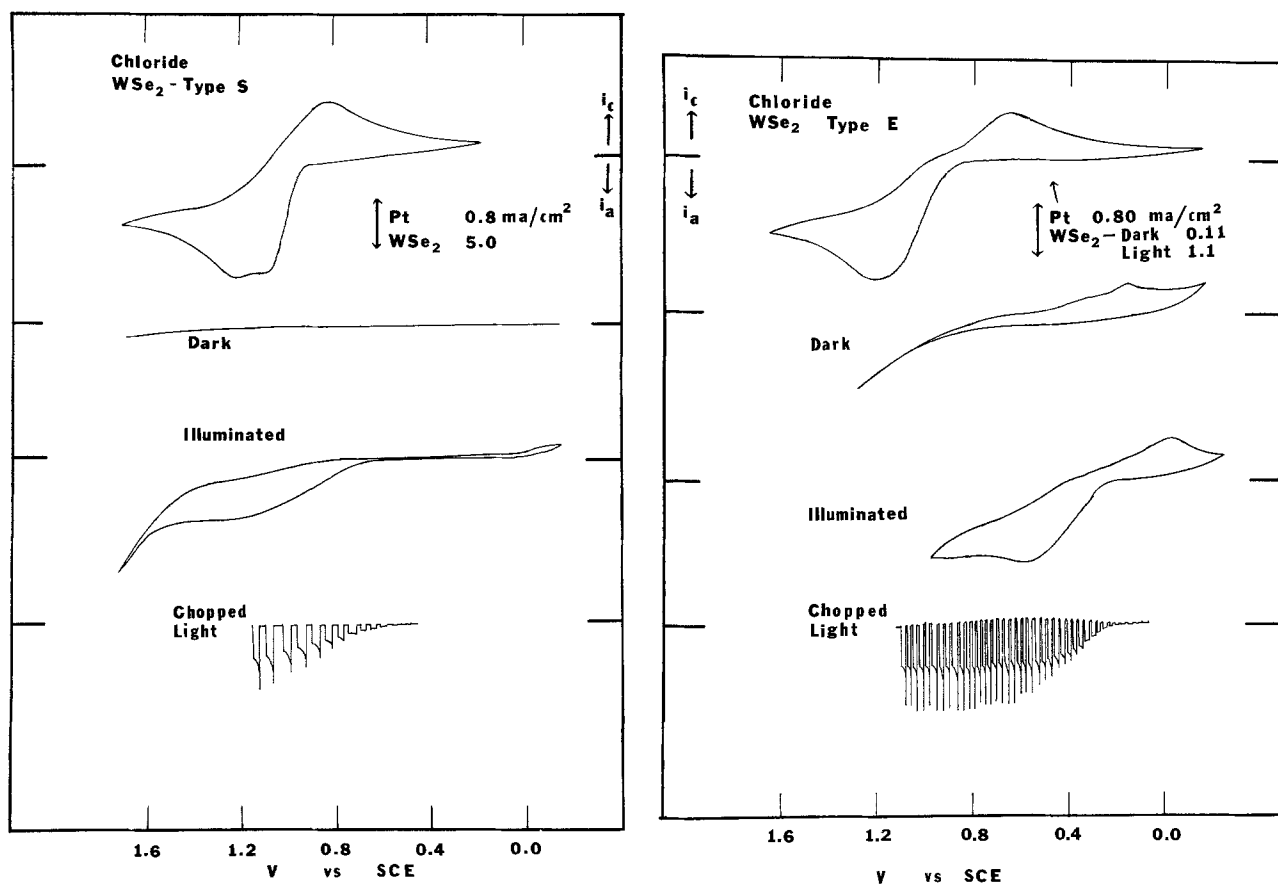


Fig. 7. Voltammetric behavior of chloride in MeCN containing 0.2M TBAP and 10 mM  $\text{Cl}^-$ . (a) Type S; (b) type E. Scan rate, 100 mV/sec except for chopped light scan at 10 mV/sec.

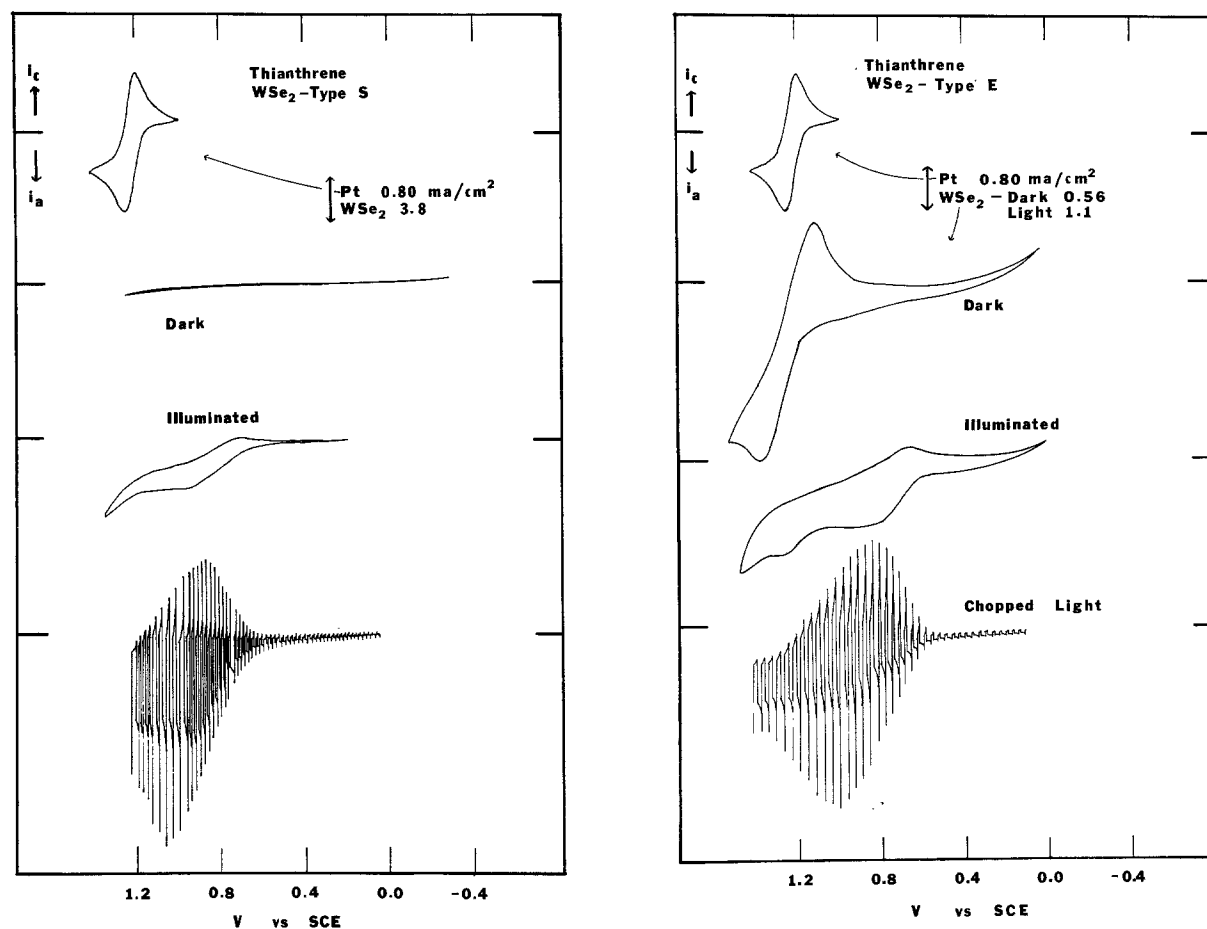


Fig. 8. Voltammetric behavior of thianthrene in acetonitrile solution containing 0.2M TBAP and 5 mM Th. (a) Type S; (b) type E. Scan rate, 100 mV/sec except for chopped light scan at 10 mV/sec.

Irradiation of the  $\text{WSe}_2$  photoanode with the full output from a 450W xenon lamp ( $>590$  nm and infrared filtered) focused onto the electrode surface yielded the  $i_{sc}$  and  $V_{oc}$  values listed in Table IV. Maximum power efficiencies under these conditions were estimated to be 7%–10.5%. No attempts were made to correct for solution absorption or reflections at the cell windows or the electrode surface. However, since the same photocurrent was found at  $\sim 80\%$  of this light intensity, the power efficiencies at lower intensities would be  $\sim 2\%$  higher.

The stability of n- $\text{WSe}_2$  (type S) against possible attack by  $\text{Cl}_2$  generated at the surface was tested by allowing the photovoltaic cell to run for several hours (Fig. 14). After 7 hr, the short-circuit photocurrent had decreased by  $\sim 4\%$  from its original stable value of 146  $\mu\text{A}$ . This corresponds to 3.7C of charge passed which represents an amount of charge sufficient to consume an appreciable part of the 10 mg crystal, if corrosion were occurring. The electrode surface appeared unchanged after 7 hr.

Table IV. Characteristics of several photovoltaic cells: n- $\text{WSe}_2$  (type S)/(MeCN),  $\text{Cl}^-$ ,  $\text{Cl}_2/\text{Pt}^+$

Electrode**	Conc. TEACl	Fill factor (max)	Power efficiency	$i_{sc}$ (mA/cm <sup>2</sup> )	$V_{oc}$ (mV)
A	Satd.	0.27	6.4	70	510
A	1.9M	0.24	5.6	65	540
B	Satd.	0.26	10.4	125	480
C	Satd.	0.23	7.6	120	410
C	1.9M	0.28	10.3	96	575
D	Satd.	0.20	7.3	90	544

\* Irradiated with light  $>590$  nm. The power output of the lamp was 150 mW/cm<sup>2</sup>.

\*\* Electrodes A-D were different type S crystals.

## Discussion

**Dark and photocurrents.**—The large differences in dark currents on the type S and type E electrode can be understood by a modified model used by Gerischer *et al.* for dark currents on  $\text{MoS}_2$  (15). In this model, the d-orbitals parallel to the C-axis, in addition to forming the conduction band in the bulk material, are assumed to provide surface states at discontinuities of the type E electrode at energies in the upper part of the bandgap (11). Facile electron transfers can take place from the electroactive species into the conduction band via these mediating d-orbitals. When the exposed surface is free from edges, the layer of Se atoms block overlap between the conduction band and molecular orbitals of the species. In this case, electron transfer in the dark via the conduction band is allowed only by thermal excitation or by tunneling. This model seems to fit the behavior found for the oxidation of Th at  $\text{WSe}_2$ . In the dark, a small current ( $<0.2$  mA/cm<sup>2</sup>) is observed on the type S electrodes. This dark current is no larger than the current observed for the same electrode in a solution containing only supporting electrolyte (0.2M TBAP). At the type E electrode, a large, mass transfer limited, dark current is observed for Th oxidation indicating that the current is not controlled by the number of dark oxidation sites on the crystal surface. Under illumination, both electrodes show similar voltammetric responses, with slightly higher photocurrents observed on the type S electrode. Thus for the type E electrode, the existence of the surface states allows Fermi level pinning and electron transfer to occur at potentials close to the standard potential of the redox couple. However, for a type S electrode, there are much lower densities of surface states near the conduction band. Fast electron transfer reactions do not occur in the dark for couples with potentials much more positive than the flatband

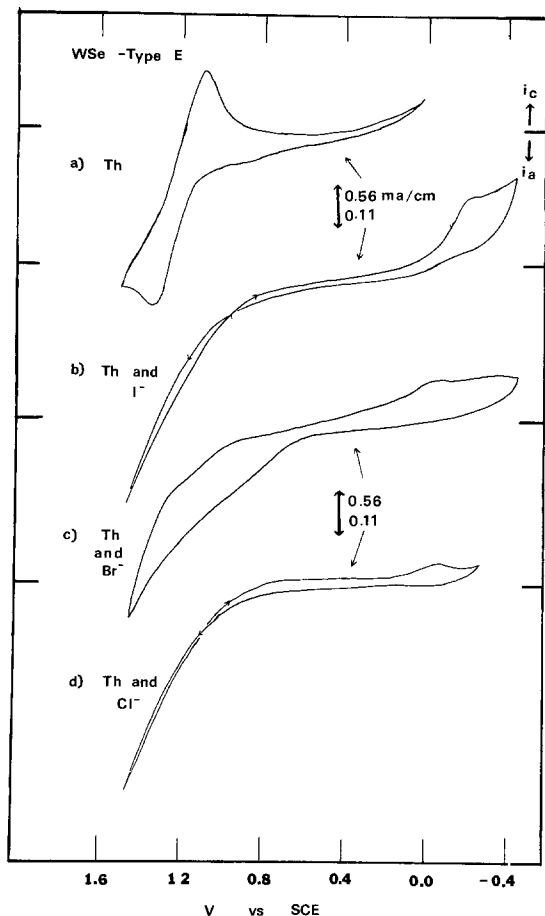


Fig. 9. Effect of bulk halide on dark currents at type E  $n$ - $WSe_2$  electrode. (a) 5 mmoles thianthrene (Th); (b) 5 mmoles Th and 15 mM TBAI; (c) 5 mM Th and 10 mM TBABr; (d) 5 and 10 mM TMACI. Scan rate 100 mV/sec. 0.2M TBAP as the supporting electrolyte.

potential. However, even with type S electrodes, Fermi level pinning at the bottom part of the bandgap may occur, as discussed later.

The photo-oxidation of halide species shows a slightly more complicated behavior. At the type S electrode, the dark anodic current in the presence of halides is about the same as the small dark current observed in a solution containing only supporting electrolyte. However, at the type E electrode, the dark current in the presence of halides is much smaller than that in the blank solution. Tributsch *et al.* have previously proposed an interaction of  $I^-$  with the surface in aqueous solutions (5f). The decrease in the dark oxidation currents on the type E electrode on the addition of halide ions similarly suggests a strong interaction of  $I^-$ ,  $Br^-$ , and  $Cl^-$  with the surface states, composed of empty d-orbitals along the exposed edges, deactivating these previously dark active sites. This is confirmed by the decrease in the dark currents for Th oxidation (and Th $\cdot$  reduction) by the addition of  $I^-$ ,  $Br^-$ , or  $Cl^-$ .

The total photocurrent densities for the oxidation of  $Cl^-$  or  $Br^-$  are 3-5 times larger at the type S electrode. Apparently while the dark active sites at the exposed edges are ineffective for the dark oxidation of  $Br^-$  or  $Cl^-$ , they remain rather efficient at trapping electrons and reducing photogenerated  $Cl_2$  and  $Br_2$ . The total photocurrent density for the oxidation of  $I^-$  at the two electrodes was approximately the same.

The difference in behavior between  $Br^-$  or  $Cl^-$  and  $I^-$  probably reflects the stronger interaction of  $I^-$  with the electrode surface. The decrease in background current after treatment with halide (compare the dark

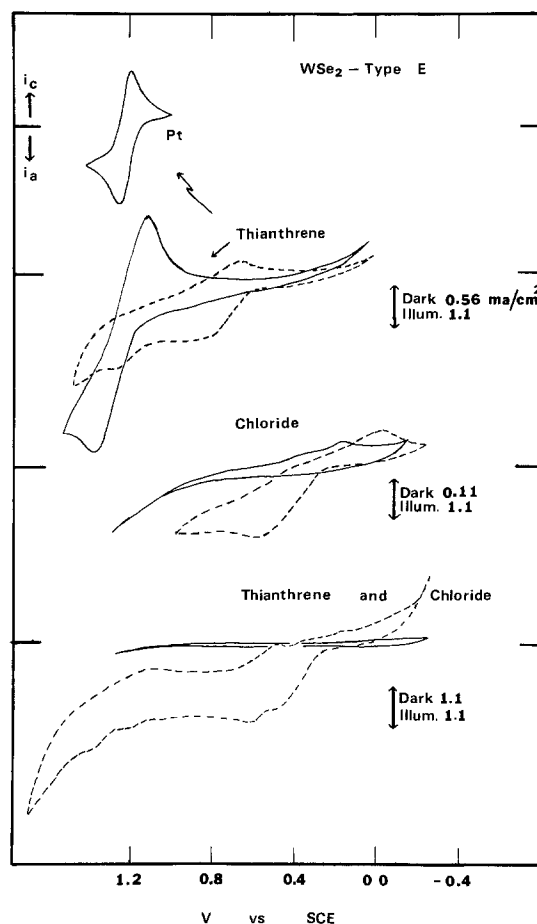


Fig. 10. Effect of chloride on photo-oxidation of thianthrene; 5 mmoles Th, 10 mM TEACI, and 0.2M TBAP in acetonitrile solution. Solid lines indicate dark current; broken lines indicate photocurrent; same conditions of Th and  $Cl^-$  in mixed solution.

currents at type E electrode before and after addition of  $I^-$ ,  $Br^-$ ,  $Cl^-$ ) is important, since this current is presumably caused by oxidation of the surface lattice in the presence of trace amounts of  $H_2O$  in the acetonitrile (5e). Suppression of the crystal oxidation is equivalent to stabilization of these photoanodes and may be the reason for the stability observed in the aqueous iodide (5e, 9) and nonaqueous chloride (6, 7) cells employing layered materials. Further experiments are necessary to demonstrate if the halide pre-treatments are sufficient for long-term stability.

**Photopotentials.**—From differential capacitance measurements,  $V_{FB}$  of  $n$ -type  $WSe_2$  (both type S and E) in MeCN/TBAP alone was  $-0.3 \pm 0.1V$  vs. SCE (Table II). The bandgap of these samples, determined from the action spectrum, is  $\sim 1.4$  eV. After correction for the difference between Fermi level and the conduction band edge, this places the edge of the valence band at  $\sim 1.0V$  vs. SCE. This is in good agreement with the flat-band potential of  $p$ -type  $WSe_2$ ,  $+1.0V$  vs. SCE, measured in MeCN (16).

The difference in potential for oxidation at Pt and illuminated  $WSe_2$  (i.e., the photounderpotential) vs. the standard potential for several redox couples is shown in Fig. 15. The standard potentials taken for  $I^-$ ,  $Br^-$ , and  $Cl^-$  are the average of the reduction and oxidation peak potentials at Pt. The  $V_{on}$  for  $I^-$  and  $Br^-$  is approximately 0.2-0.3V positive of the measured flat-band potential. This positive value of  $V_{on}$  suggests recombination is occurring and this can be attributed to the band of surface states lying directly below the conduction band edge.

For couples with standard potentials more positive than 0.5V vs. SCE ( $Cl^-/Cl_2$ , Th/Th $^+$ , and Ru(bpy) $_3^{2+/3+}$ ) the photopotential ( $V^\circ - V_{on}$ ) be-



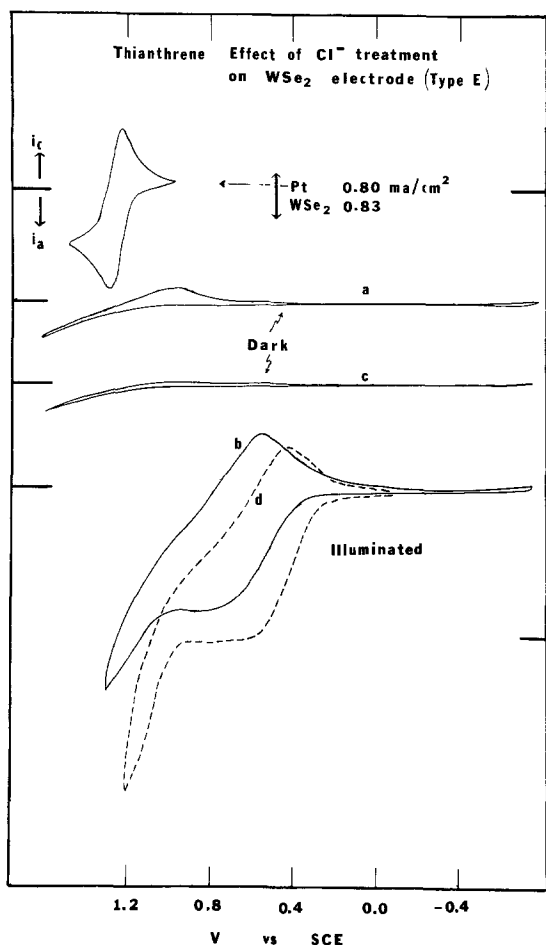


Fig. 11. Effect of dipping type E n-WSe<sub>2</sub> electrode into 7 mM TEACl solution. (a) Dark oxidation of 5 mM Th on untreated electrode. (b) Photo-oxidation of 5 mM Th on untreated electrode. (c) Dark oxidation of Th after Cl<sup>-</sup> treatment. (d) Photocurrent after Cl<sup>-</sup> treatment.

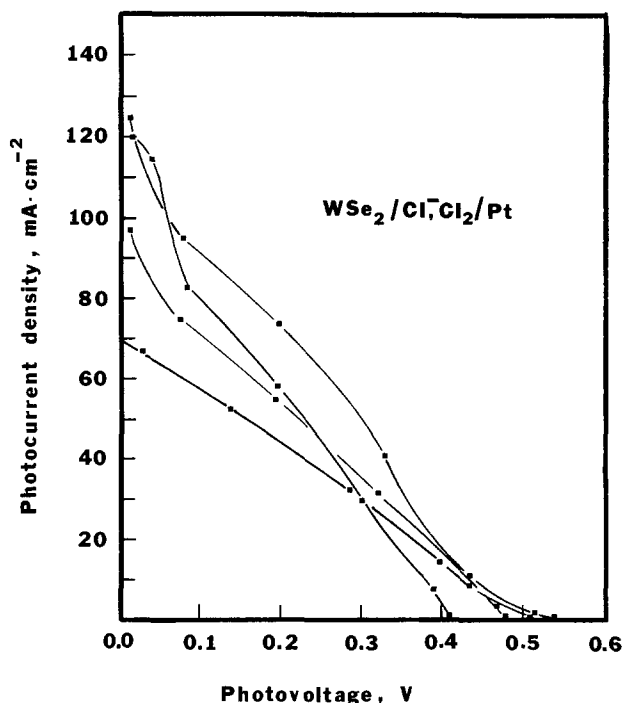


Fig. 12. Performance characteristics of n-WSe<sub>2</sub>/Cl<sup>-</sup> (satd.), Cl<sub>2</sub>/Pt photoelectrochemical cells. 450W Xe lamp fitted with a 590 nm cut-on filter used as light source. Power of focused light at electrode surface, 150 mW/cm<sup>2</sup>.

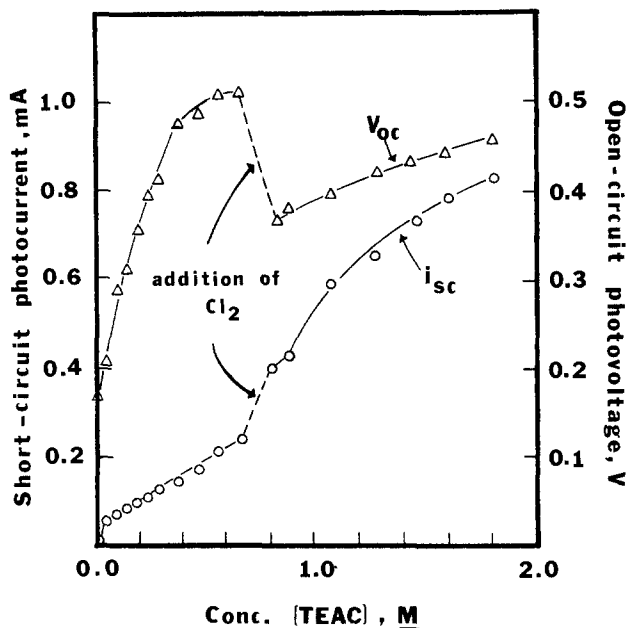


Fig. 13. Effect of Cl<sup>-</sup> and Cl<sub>2</sub> concentration on open-circuit photovoltage,  $V_{oc}$ , and short-circuit photocurrent,  $i_{sc}$ . Electrode area, 0.011 cm<sup>2</sup>. Light source as in Fig. 12.

comes almost constant at a value of  $\sim 0.4\text{-}0.5\text{V}$ . This limiting value can best be understood by Fermi level pinning (2a) at surface states located approximately 0.5 eV above the valence bandedge.  $V_{on}$  for redox couples with  $V^\circ$  more positive than 0.5V vs. SCE should increase linearly with increasing  $V^\circ$ . For couples with  $V^\circ$  at potentials negative of the surface-state level ( $<0.5\text{V}$ ),  $V_{on}$  is constant and the photopotential should increase as  $V^\circ$  becomes more positive, as seen in Fig. 15. Further evidence for the presence of surface states is the highly dependent nature of the photovoltage developed in the n-WSe<sub>2</sub>/Cl<sup>-</sup>, Cl<sub>2</sub>(MeCN)/Pt cell upon the Cl<sub>2</sub>/Cl<sup>-</sup> ratio (Fig. 13). Based on the ideal model of the semiconductor-solution interface (1),  $V_{on}$  should be at  $V_{FB}$  and the Pt electrode would be poised by the redox couple so that a higher photovoltage is expected with higher Cl<sub>2</sub>/Cl<sup>-</sup> ratios, i.e., a higher Cl<sub>2</sub>/Cl<sup>-</sup> shifts the solution redox potential to more positive values while the bandedges remain unaffected. However, the experimental results do not conform to this behavior. Upon addition of Cl<sub>2</sub>,  $V_{oc}$  actually decreases (see Fig. 13). This could be attrib-

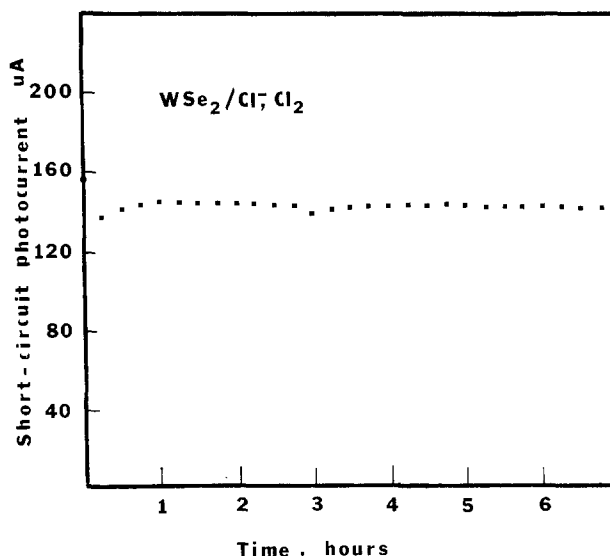


Fig. 14. Short-circuit photocurrent of WSe<sub>2</sub>/Cl<sup>-</sup> (1.9M), Cl<sub>2</sub>/Pt PEC cell as function of time. Electrode area, 0.015 cm<sup>2</sup>.

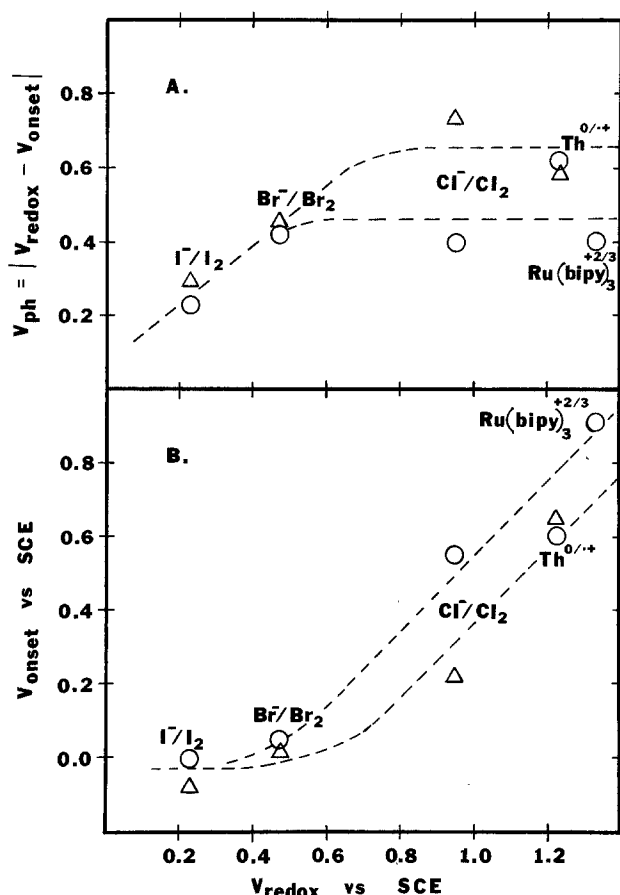
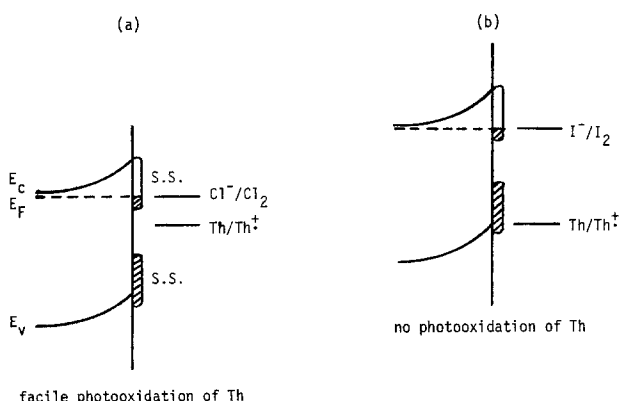


Fig. 15. (a) Comparison of photopotentials developed at type S (O) and type E ( $\Delta$ ) WSe<sub>2</sub> electrode for several redox couples in MeCN. (b) Comparison of onset potential of photocurrent at type S (O) and type E ( $\Delta$ ) electrodes for several redox couples in MeCN.

uted to a higher surface recombination rate at the higher Cl<sub>2</sub> concentration.

The shift in onset potential for Th oxidation at the type E electrode in the presence of Cl<sup>-</sup> can also be explained by Fermi level pinning as shown in Scheme I (a). As the applied potential is biased in a positive direction, Cl<sub>2</sub> is initially generated and the Fermi level is pinned at the redox potential of Cl<sub>2</sub>/Cl<sup>-</sup> or, more likely, somewhat between the V<sup>o</sup>'s of the two redox couples. The result should be a more negative onset potential for thianthrene oxidation as is observed in Fig. 10. I<sup>-</sup>/I<sub>2</sub> does not affect the onset potential for thianthrene oxidation, since at the potential where the Fermi level is pinned, i.e., at the standard potential of I<sup>-</sup>/I<sub>2</sub>, the valence bandedge and the bottom surface



Scheme I. E<sub>C</sub>, conduction bandedge; E<sub>F</sub>, Fermi level; E<sub>V</sub>, valence bandedge; S.S., surface state.

states are well beyond the potential of Th/Th<sup>+</sup> [see Scheme I (b)].

### Conclusion

The results presented here indicate that the surface morphology of WSe<sub>2</sub> single crystals is a critical factor in determining their performance characteristics in photoelectrochemical cells. Both the photocurrent and photovoltage are dependent on the discontinuities in the surface plane. The application of layer-type semiconductors toward efficient solar conversion devices will depend on the ability to passivate recombination centers located at these surface discontinuities. Halide pretreatment can improve the photoresponse for the oxidation of thianthrene. Surface pretreatments with other electron-donating species may passivate recombination to a larger degree and is under investigation. The correlation of the density of surface states (surface discontinuities) with the observed photopotential lends support to the role of Fermi level pinning (2). Further results are required before an unambiguous relationship can be drawn between the density of surface states and the observed photopotential.

The stability and efficiency of the nonaqueous n-WSe<sub>2</sub>/Cl<sup>-</sup>, Cl<sub>2</sub>/Pt photovoltaic cell confirm the original predictions of Tributsch (5a) on the performance of layered materials.

### Acknowledgment

The assistance of Dr. Michael Schmerling in obtaining the electron micrographs is gratefully appreciated. This work was supported by the National Science Foundation, the Office of Naval Research, and by the Solar Energy Research Institute (in a cooperative project with SumX Corporation).

Manuscript submitted Aug. 19, 1980; revised manuscript received Dec. 1, 1980.

Any discussion of this paper will appear in a Discussion Section to be published in the December 1981 JOURNAL. All discussions for the December 1981 Discussion Section should be submitted by Aug. 1, 1981.

Publication costs of this article were assisted by The University of Texas.

### REFERENCES

- H. Gerischer, in "Physical Chemistry: An Advanced Treatise," H. Eyring, D. Henderson, and W. Jost, Editors, Vol. 9A, Academic Press, New York (1970).
- (a) A. J. Bard, A. B. Bocarsly, F.-R.F. Fan, E. G. Walton, and M. S. Wrighton, *J. Am. Chem. Soc.*, **102**, 3671 (1980); (b) F.-R.F. Fan and A. J. Bard, *ibid.*, **102**, 3677 (1980); (c) A. B. Bocarsly, D. C. Bookbinder, R. N. Dominey, N. S. Lewis, and M. S. Wrighton, *ibid.*, **102**, 3683 (1980).
- (a) R. Memming and G. Schwandt, *Surf. Sci.*, **5**, 97 (1966); (b) R. A. L. Vanden Berghe, F. Cardon, and W. P. Gomes, *ibid.*, **39**, 368 (1973); (c) P. Kohl and A. J. Bard, *J. Am. Chem. Soc.*, **99**, 7531 (1977); (d) S. Frank and A. J. Bard, *ibid.*, **97**, 7427 (1975).
- (a) B. A. Parkinson, A. Heller, and B. Miller, *J. Appl. Phys.*, **33**, 521 (1978); (b) B. A. Parkinson, A. Heller, and B. Miller, *This Journal*, **126**, 954 (1979).
- (a) H. Tributsch, *Z. Naturforsch. Teil A*, **32**, 972 (1977); (b) H. Tributsch and J. C. Bennett, *J. Electroanal. Chem. Interfacial Electrochem.*, **81**, 97 (1977); (c) H. Tributsch, *Ber. Bunsenges. Phys. Chem.*, **81**, 361 (1977); (d) H. Tributsch, *ibid.*, **82**, 169 (1978); (e) H. Tributsch, *This Journal*, **125**, 1086 (1978); (f) H. Tributsch, H. Gerischer, C. Clemen, and E. Bucher, *Ber. Bunsenges. Phys. Chem.*, **83**, 655 (1979); (g) J. Gobrecht, H. Gerischer, and H. Tributsch, *This Journal*, **125**, 2085 (1978).
- L. F. Schneemeyer and M. S. Wrighton, *J. Am. Chem. Soc.*, **101**, 6496 (1979).
- L. F. Schneemeyer, M. S. Wrighton, A. Stacy, and

- M. J. Sienko, *Appl. Phys. Lett.*, **36**, 701 (1980).
8. L. F. Schneemeyer and M. S. Wrighton, *J. Am. Chem. Soc.*, Submitted.
  9. F.-R. F. Fan, H. S. White, B. Wheeler, and A. J. Bard, *J. Am. Chem. Soc.*, **102**, 5142 (1980); *This Journal*, **127**, 518 (1980).
  10. H. J. Lewerenz, A. Heller, and F. J. DiSalvo, *J. Am. Chem. Soc.*, **102**, 1877 (1980).
  11. W. Kautek, H. Gerischer, and H. Tributsch, *Ber. Bunsenges. Phys. Chem.*, **83**, 1000 (1979).
  12. N. E. Tokel-Takvoryan, R. E. Hemingway, and A. J. Bard, *J. Am. Chem. Soc.*, **95**, 6582 (1973).
  13. S. N. Frank, A. J. Bard, and A. Ledwith, *This Journal*, **122**, 898 (1975).
  14. A. R. Beal, W. Y. Liang, and H. P. Hughes, *J. Phys. C*, **9**, 2449 (1976).
  15. S. M. Ahmed and H. Gerischer, *Electrochim. Acta*, **24**, 705 (1979).
  16. G. Nagasubramanian and A. J. Bard, *This Journal*, **128**, 1055 (1981).

## Semiconductor Electrodes

### XXXIV. Photoelectrochemistry of p-Type $\text{WSe}_2$ in Acetonitrile and the p- $\text{WSe}_2$ -Nitrobenzene Cell

G. Nagasubramanian and Allen J. Bard\*

Department of Chemistry, University of Texas at Austin, Austin, Texas 78712

#### ABSTRACT

The photoelectrochemical behavior of p-type  $\text{WSe}_2$  single crystal electrodes in acetonitrile solutions containing a number of redox couples [e.g., N,N,N',N'-tetramethyl-p-phenylene diamine (+ 1/0), methyl viologen (+ 2/+1), nitrobenzene (0/-1), phthalonitrile (0/-1)] was investigated. For couples with potentials in the bandgap region (ca. -0.4 to +1.0V vs. SCE), a linear increase of the photopotential with  $V_{\text{redox}}$  was observed. Couples located at more negative potentials (i.e., above the conduction band edge) also showed a photoeffect, with the photopotential pinned at  $\sim -0.95\text{V}$ ; this was ascribed to surface state pinning or inversion. A PEC cell of the form p- $\text{WSe}_2/\text{PhNO}_2$ , MeCN/Pt is described. Treatment of the p- $\text{WSe}_2$  electrode with iodide was shown to improve the efficiency of such cells.

In the preceding paper, the behavior of n-type  $\text{WSe}_2$  in acetonitrile (MeCN) solutions was discussed (1).  $\text{WSe}_2$  and other layer-type semiconductor materials, first proposed by Tributsch for photoelectrochemical (PEC) applications (2), have been extensively investigated recently (3-8). The results with n- $\text{WSe}_2/\text{MeCN}$  were consistent with a flatband potential of  $\sim -0.3\text{V}$  vs. SCE and the existence of surface states which provide sites for surface recombination and lead to Fermi level pinning. Studies of p-type  $\text{WSe}_2$  in MeCN were undertaken to confirm the location of the band edges in  $\text{WSe}_2$  and to ascertain if the behavior of a number of redox couples at this material was consistent with a pinning model.

A second goal of this work was the construction of a PEC cell for conversion of solar to electrical energy utilizing this material. Past research involving PEC cells in nonaqueous solvents such as MeCN have shown that while high stability can often be attained in such systems, the maximum light intensities that can be utilized are often limited by the low concentrations of the electroactive materials in the solution (9). However, nitrobenzene ( $\text{PhNO}_2$ ) is miscible in all proportions with MeCN and should be a reasonable oxidant at a p-type semiconductor electrode. Cells with p- $\text{WSe}_2$  and  $\text{PhNO}_2$  which appear stable and show monochromatic efficiencies  $\sim 4\%$  are described here.

#### Experimental

**Chemicals.**—Nitrobenzene ( $\text{PhNO}_2$ ) was purified following the procedure of Marcoux *et al.* (10).  $\text{PhNO}_2$  was first passed through an activated alumina column and then vacuum distilled. MeCN was purified as previously described (11). The other redox couples were purified by recrystallization. All compounds were stored inside a helium-filled Vacuum Atmosphere Cor-

poration (Hawthorne, California) glove box. Polarographic grade, tetra-n-butyl ammonium perchlorate (TBAP), dissolved and recrystallized from ethanol, thrice, and dried under vacuum ( $<10^{-5}$  Torr) for 3 days was used as supporting electrolyte. The cell employed was a conventional single compartment cell of 25 ml capacity containing the p- $\text{WSe}_2$ , a Pt working and counterelectrode and a quasi-reference electrode, which was an Ag wire immersed inside the solution and separated from it by a medium-porosity glass frit. The potential of this electrode was checked against an aqueous saturated calomel electrode (SCE) at regular intervals and was found to be constant. All potentials, unless specified otherwise, are given in V vs. SCE.

The p- $\text{WSe}_2$  single crystal generously donated by Dr. B. Miller and Dr. F. DiSalvo, Bell Laboratories, was used as the electrode. This was selected, after carefully verifying under microscope that the surface was quite free of exposed edges. A clean new crystal surface ( $\perp$  C-axis) was produced by attaching adhesive tape and peeling off the surface layer. Gold was electroplated on one side of the pellet and the contact was found to be ohmic. A copper wire lead for electrical contact was attached to the gold-coated side with silver epoxy cement (Allied Product Corporation, New Haven, Connecticut) and was subsequently covered with 5 min epoxy cement. The assembly was mounted into 7 mm diam glass tubing and was held in position with silicone rubber sealant (Dow Corning Corporation, Midland, Michigan), which also served as an effective seal against the seepage of electrolyte solution to the rear of the semiconductor electrode. The exposed area of p- $\text{WSe}_2$  was  $0.05\text{ cm}^2$ . The surface of the electrode was etched before use with 12M HCl for 5-10 sec and then rinsed thoroughly with distilled water and dried. The area of the Pt cylindrical wire, used as a counterelectrode, was  $0.15\text{ cm}^2$ .

\* Electrochemical Society Active Member.  
Key words: capacitance, voltammetry, solar cells.